Destruction of a fluvial reservoir by hydrothermal activity (Cameros Basin, Spain)

M. Ochoa [a,*], J. Arribas [a], R. Mas [b], R.H. Goldstein [c]

[a] *Departamento de Petrología y Geoquímica, Universidad Complutense de Madrid, Facultad de Ciencias Geológicas, C/ José Antonio Novais 2, 28040, Madrid, Spain*

[b] *Departamento de Estratigrafía, Universidad Complutense de Madrid, Facultad de Ciencias Geológicas, C/ José Antonio Novais 2, 28040, Madrid, Spain*

[c] *Department of Geology, University of Kansas 1475 Jayhawk Boulevard, 120 Lindley Hall, Lawrence, Kansas 66045-7613, USA*

Abstract

This study provides an example of a high-quality fluvial hydrocarbon reservoir that was completely destroyed by hydrothermal processes. The reservoir unit was deposited in the Cameros Basin, located in the NW sector of the Iberian Chain (Spain). The basin was filled with clastic fluvial deposits (sandstones and conglomerates) between Late Berriasian and Early Aptian times. Provenance of sands was mainly from coarse crystalline rocks. A humid tropical climate produced intense weathering of K-feldspar during transport from source to basin. Thus, a mineralogically mature rigid framework with high porosity existed at the time of deposition, which would have constituted a high-quality hydrocarbon reservoir. At present however, the porosity of the reservoir is negligible. Porosity was reduced by a sequence of diagenetic processes: (1) mechanical compaction (i.e. crushing of metamorphic lithic grains) and chemical compaction, (2) kaolinite and siderite cementation, and (3) early quartz cementation. Hydrocarbon emplacement probably occurred between phases (2) and (3). A low-grade metamorphic (hydrothermal) event, reaching greenschist facies, took place during the Late Cenomanian. It dramatically reduced the remaining porosity of the reservoir and destroyed the hydrocarbon charge. Hydrothermal processes which affected the sandstones include (1) re-compaction; (2) late quartz cementation and silicification of remaining feldspars; (3) carbonate cementation; (4) chloritization of feldspars, metamorphic lithic fragments and intrabasinal argillaceous grains; and (5) growth of pyrite and chloritoid crystals on argillaceous material of intrabasinal, extrabasinal or even diagenetic origin. Hydrocarbons that migrated to the margins of the basin escaped these hydrothermal modifications and were preserved. The results of this study may be used to predict the diagenetic and hydrothermal evolution of other potential reservoirs in similar tectonic settings.

Keywords: Sandstone diagenesis; Hydrothermal activity; Metamorphism; Porosity reduction; Cameros Basin; Spain

1. Introduction

Among the Mesozoic basins of the Iberian Chain (Spain), the Cameros Basin preserves the most complete sedimentary record of the time interval from the Tithonian to the Early Albian (Fig. 1). During this period, the anomalously high subsidence and sedimentation rates within the basin produced a sedimentary record that reached up to 5 km in vertical thickness (representing up to 9 km of stratigraphic record in the direction of the northward migration of the successive depositional sequences which filled the basin). Two sectors with different features can be distinguished: the

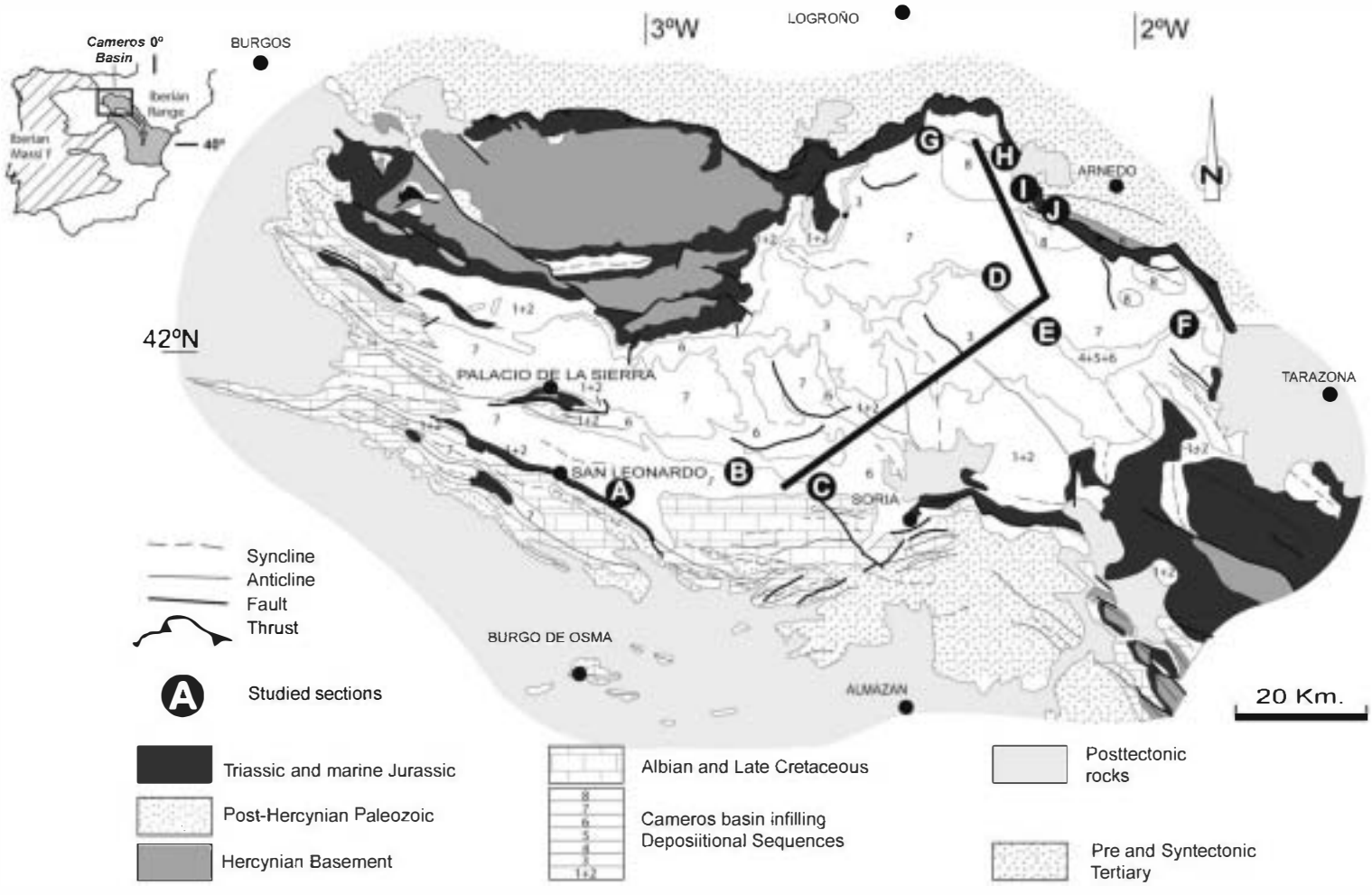

Fig. 1. Simplified geologic map showing study area and location of the transect through the outcrops. The stratigraphic sections are located in Muriel (A), Cidones-Abejar (B), Golmayo (C), Yanguas (D), San Pedro Manrique (E), Valdemadera (F), Trevijano (G), Jubera (H), Ameallo (I) and Préjano (J).

northeastern sector, characterized by the most rapid rates of subsidence and affected by low-grade (hydrothermal) metamorphism; and the southwestern sector, characterized by the presence of secondary depocenters and unaffected by metamorphism.

The focus of this study is the northern and central part of the eastern Cameros Basin (Fig. 1, outcrops from D to J). A SW–NE trending geological cross-section from this area is shown in Fig. 2. In this area, Mas et al. (2003) described eight depositional sequences (DS) ranging in age from Tithonian to Early Albian (Fig. 3). This study is focused on the maximum syn–rift filling stage (DS-4 to DS-7), from Late Berriasian to Early Aptian (Urbión Group), in which a succession of up to 2.2 km of clastic sediments was formed.

Although there are many publications dealing with stratigraphy, sedimentology and mineralogy of the Urbión Group (e.g. Salinas and Mas, 1989; Casquet et al., 1992; Mas et al., 1993; Alonso-Azcárate et al., 1995; Mantilla et al., 1998; Alonso-Azcárate et al., 1999a,b; Barrenechea et al., 2001; Mata et al., 2001; Mantilla et al., 2002; Mas et al., 2003), little attention has been paid to reservoir characterisation and evaluation of these clastic sediments (Arribas et al., 2003). The petroleum systems of the basin are discussed by Mas et al. (2002). The absence of hydrocarbons in the basin fill prompted the present analysis of the metamorphic (hydrothermal) processes that caused their destruction.

This paper documents the destructive effects of burial diagenesis and low-grade hydrothermal metamorphism on reservoir quality, and provides insights into the evolution of hydrocarbon reservoirs in other basins affected by these processes. Hydrothermal alteration of clastic reservoirs has been frequently documented (i.e., Hoffman and Hower, 1979; Larese, 1997). Common related processes include mineral cementation and recrystallization, generated by acid hot water flows, which promotes porosity/permeability reduction (i.e., Oelkers et al., 1996; De Ros et al., 2000). Low-grade hydrothermal metamorphism may produce a complete occlusion of fluid pathways in the reservoir (Dutkiewicz et al., 1995; Buick et al., 1998). In many basins hydrothermal metamorphism develops locally, and preservation of economically exploitable reservoirs may occur in areas of the basin unaffected by metamorphism (Spötl et al., 1994; Pittman and Spölt, 1996; Spötl et al., 2000). Thus, understanding the processes that

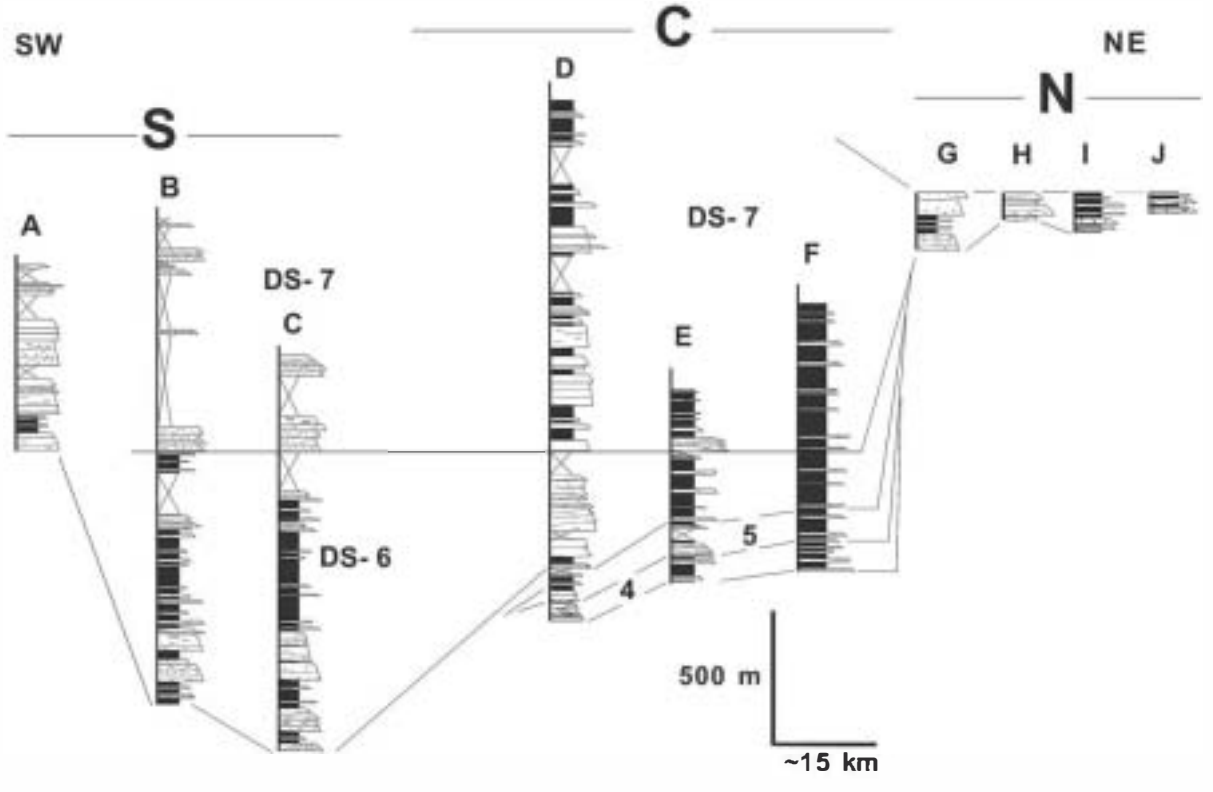

Fig. 2. Stratigraphic transect of Urbión Group through the southern area (S), central area (C) and northern area (N) of the basin. See Fig. 1 for location of sections.

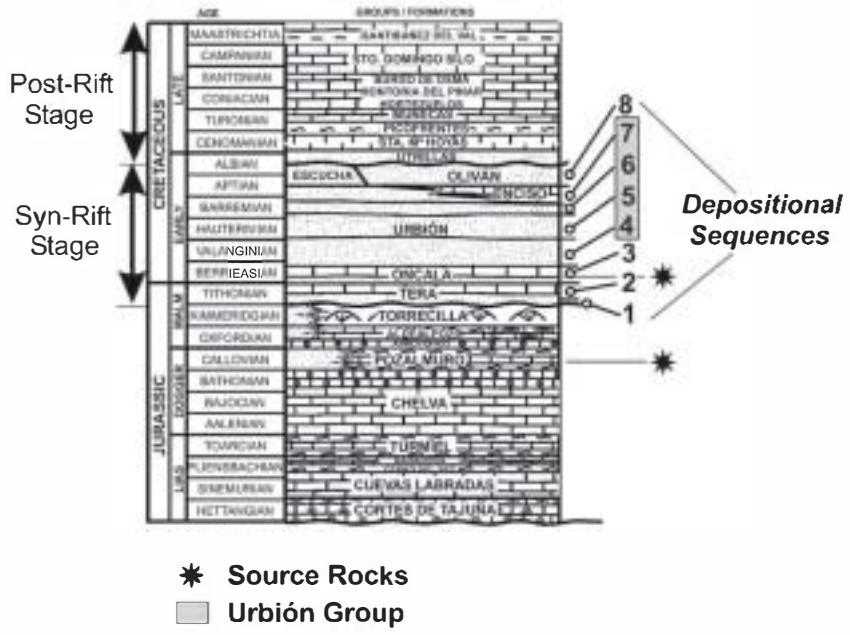

Fig. 3. Rift and post-rift stages in the evolution of the Iberian Basin (Modified from Salas et al., 2001) and idealised stratigraphic section showing the latest Paleozoic and Mesozoic sratigraphic record in the Cameros area.

affected "palaeo-reservoir" quality is an important objective in predictive diagenetic reservoir modelling.

2. Geological setting

The Cameros Basin is an intracratonic basin, representing a folded segment of the Alpine Chain that developed as a consequence of the contractional inversion of the Mesozoic Iberian rift basin. The development of this basin took place in two phases: the first phase lasted from Early Permian to the Late Triassic and the second from Tithonian to Early Albian. These two rifting phases were followed by post-rift thermal subsidence, during which mainly shallow marine carbonates were deposited (Guimerà et al., 1995; Salas et al., 2001) (Figs. 1–3).

During the second stage of rifting, a thick succession (<5 km total thickness) of alluvial to lacustrine, depositional sequences was accumulated in the depocentre of the Cameros Basin (Fig. 3). According to Mas et al. (2003), the basin fill constitutes a large megasequence bounded by two main unconformities (Fig. 3). The megasequence can be subdivided into eight depositional sequences (DS-1 to 8); this study focused on the interval between DS-4 and DS-7, which constitutes the Urbión Group.

The thickness of the Urbión Group varies dramatically from 100 m in the marginal areas of the basin to 2200 m in the depocentres (Fig. 2). It comprises sandstones and conglomerates interbedded with shales, which were deposited in settings ranging from braided systems (Mas et al., 2003) in the southwestern area of the basin (A to C in Fig. 1) to meandering fluvial and lacustrine systems (Mas et al., 2003) in the central and northeastern areas (D to F in Fig. 1); and alluvial-fan facies (Mas et al., 2003) in the northern part of the basin (G to J in Fig. 1).

3. Basin evolution, potential source rocks and metamorphism

Mas et al. (2003) summarized the genesis and evolution of the Cameros Basin (Fig. 4). Extensive carbonate platforms developed during Jurassic times, i.e., before the Tithonian to Early Albian rifting phase (1, in Fig. 4). The Cameros Trough began to form as an extensional ramp basin from Tithonian to Berriasian time. Depositional Sequences 1 to 3 were deposited in this time interval (2, in Fig. 4). The maximum thickness of strata is reached in the DS-4 to DS-8 deposits of the central zone, corresponding to the time interval of maximum extension from Berriasian to Early Albian. This initiated organic matter maturation and hydrocarbon migration towards permeable units in the basin (3a and 3b, in Fig. 4). Marine environments re-occupied the Cameros area during the Late Cretaceous, constituting the Post-Rift Stage 2. During Cenomanian times, hydrothermal metamorphism affected a significant volume of

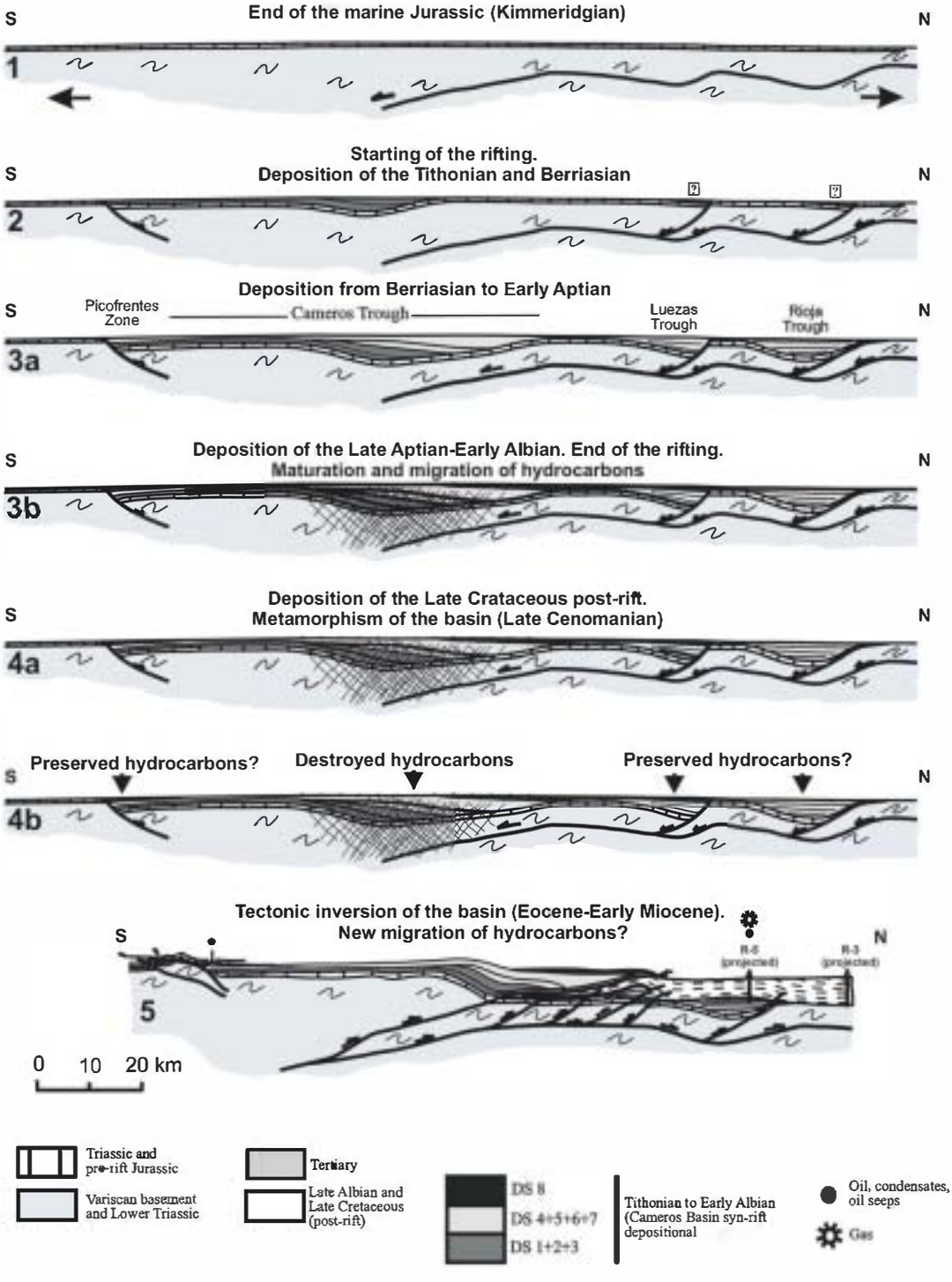

Fig. 4. Cross-sections illustrating the geological history of the Cameros Basin. See text for explanation (modified from Mas et al., 2003).

the basin fill in the Cameros Trough and hydrocarbon reservoirs were destroyed (4a and 4b, in Fig. 4). Finally, Tertiary contractional inversion of the Cameros Basin took place (5, in Fig. 4).

The potential petroleum systems of the Cameros area have been reviewed by Mas et al. (2002, 2003) based on an analysis of the Cameros Extensional Ramp Basin (Cameros Trough) depocentre and two surrounding

half-graben sub-basins (Rioja Trough to the North and Bigornia Trough to the South). The Cameros Trough is considered the central part of the Cameros Basin in which hydrothermal activity took place (Mas et al., 2003), and where early generation and migration of oil from source rocks (today over-mature) to reservoirs took place. Potential source rocks of the Cameros Trough are Callovian organic marls and black shales (type II, Tissot and Welte, 1978), Early Cretaceous lacustrine organic marls, (type II/I, Tissot and Welte, 1978), and syn-rift Early Cretaceous lignites and organic-rich shales (type III, Tissot and Welte, 1978) (Mas et al., 2003). Among the most important reservoirs were syn-rift, Early Cretaceous channelized fluvial sandstones (DS 4 to 7) (Mas et al., 2003). The rocks that represented the seals at that time were the interbedded mudstones. The timing of hydrocarbon generation can be considered as early and produced in two events: (1) Albian, during which organic matter matured by burial and (2) Late Cretaceous, during which maturation of organic matter was induced by abnormal heat flow caused by the first hydrothermal event (Mas et al., 2003). The early emplacement of hydrocarbons is supported by petrography as they predate quartz overgrowths.

The metamorphism of the basin is considered as hydrothermal and allochemical (Casquet et al., 1992; Barrenechea et al., 1995; Alonso-Azcárate et al., 1995, 2001; Mantilla et al., 2002). Two thermal events can be recognized (e.g. Mantilla et al., 2002). The first one is the most relevant here and took place after complete filling of the basin. It has been dated at the post-rift age of 106 to 86 Ma BP (from Late Albian to Coniacian). Metamorphic conditions ranged from low-grade to very low-grade, with a maximum temperature of 340–370 °C and a maximum pressure of 1 kbar (aprox. 3900 m). This hydrothermal event coincides with other regional geotectonic events such as the opening of the Gulf of Biscay (Olivet et al., 1984), and is coincident with the age of the alkaline magmatism in the Pyrenees (Montigny et al., 1986). Another hydrothermal phase has been recorded at 40 Ma (Paleogene). This phase was related to the beginning of basin inversion during the Alpine contraction.

4. Methods

Sandstone sampling was carried out in several stratigraphic sections (Figs. 1, 2). In the southern part of the basin, these sections are located at Muriel (A), Cidones-Abejar (B) and Golmayo (C). In the central part, locations of the sections are Yanguas (D), San Pedro Manrique (E) and Valdemadera (F). In the north, locations of these sections are Trevijano (G), Jubera (H), Arnedillo (I) and Préjano (J). About 150 samples of sandstone were analysed to determine clastic and authigenic products. Analytical methods included conventional petrography, fluid inclusion microthermometry, cathodoluminescence, and analyses with electron microprobe and scanning electron microscope (SEM).

For petrographic analysis, standard doubled-polished thin sections were etched and stained using HF and sodium cobaltinitrite for potassium feldspar identification, and alizarin red and potassium ferrocyanide to better distinguish carbonate components (Chayes, 1952; Lindholm and Finkelman, 1972, respectively). Four hundred points were counted per sample for quantitative petrographic analyses. The "Gazzi-Dickinson" method (Ingersoll et al., 1984) and petrographic groups defined by Zuffa (1980) were used to classify points. Post-depositional changes to the original framework were also considered and evaluated. These analyses permit a reconstruction of the original framework composition required for provenance deductions and diagenetic inferences.

Electron microprobe analysis was used to characterise carbonates cements, feldspars, clay minerals and solid fibres of hydrocarbons. Acceleration voltage and sample current intensity were set at 15 Kv and 20 nA. Standards used were TAP, LD2, PETJ, PETJH, LIF and LIFH. Many images were taken under the microprobe in backscattered light in order to recognize different brightness levels.

Double-polished thin rock slices detached from their glass mount were prepared from most samples for fluid inclusion microthermometric analysis. The thickness of the slices was between 30 and 50 μm. In all cases, cold preparation techniques were used to avoid re-equilibration of fluid inclusions (Goldstein and Reynolds, 1994). The measurements were carried out on a petrographic microscope equipped with a Linkam THMSG 600 heating and cooling stage which enables temperatures of phase transitions in the range of −180° to 300 °C. This heating stage is mounted on an Olympus BX60 polarizing microscope.

Small fragments of double-polished rock slices were also imaged under CL using an Oxford Instrument photomultifilter-based CL detector installed on a JEOL T330 SEM. Cathodoluminescence photography was performed after homogenisation temperatures had been determined in order to avoid any negative effects on data acquisition.

SEM-CL textures were used to verify that the studied fluid inclusions were located in quartz cement and not in quartz clasts, to evaluate the possibility of finding some zoning inside the quartz overgrowth itself, and also to determine the timing of quartz cementation relative to

other diagenetic processes. The latter contributed to establishing the diagenetic sequence on the basis of textural relationships.

5. Results

5.1. Petrofacies

Following the criteria of Dickinson (1985), it is possible to note a trend in framework composition from South to North (Fig. 5). In proximal zones (southern area), the sandstone composition is quartzofeldspathic (mean $Q_{81}F_{18}Lt_1$; Fig. 6A) and K-feldspar prevails over plagioclase. Sandstones from the southern part correspond to subarkoses instead of ideal arkoses due to chemical weathering in a tropical climate, which promoted a rapid decay of feldspars (Ochoa et al., 2004). These rocks evolve to more mature quartzose sandstones in depocentres (mean $Q_{96}F_3Lt_1$; Fig. 6B) suggesting significant mineralogical and textural maturation during transport over a distance of >50 km. This systematic spatial variation can also be attributed to intense weathering in a humid climate (Rat, 1982). In addition, local sources of Triassic and Jurassic sedimentary rocks (carbonate and clastics) produced quartzolithic sandstone petrofacies (mean $Q_{93}F_1Lt_6$) (Fig. 6C), in alluvial-fan environments in the northeastern part of the basin. In spite of the different petrofacies, all sandstones are considered to have an original quartz-rich rigid framework. Their mean grain-sizes range from fine to coarse. They are moderately to well sorted, which suggests that the original porosity was between 34% and 40% (Beard and Weyl, 1973). The high values of original porosity and the relatively low clay content characterize these deposits as very good reservoir rocks.

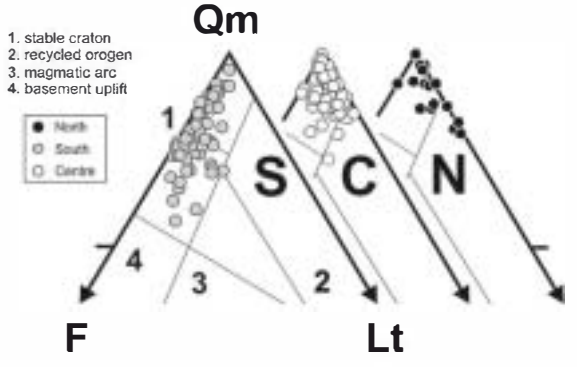

Fig. 5. Ternary plots showing sandstone petrofacies in the Urbión Group (according to Dickinson, 1985) in the southern area (S), central area (C) and northern area (N) of the basin. Qm: Monocrystalline quartz; F: K-feldspar; Lt: total lithic population.

5.2. Diagenetic and hydrothermal processes and products

Urbión Group sandstones experienced intense diagenesis. The most relevant processes are indicated in Fig. 8.

5.2.1. Compaction

Compaction has been evaluated following the criteria of Houseknecht (1987) and Lundegard (1992) for estimation of the intergranular volume of the original sediment and its reduction during diagenesis. Porosity loss by compaction (COPL, Lundegard, 1992) in the analyzed sandstones ranges from 11.9% to 37.29% for sandstones in the north; from 23.6% to 39.6% in the central area; and from 15.4% to 39% in the south (Table 1). Note that these values include both mechanical and chemical compaction. According to Lundegard (1992), the ICOMPACT (Compactional Index = COPL/(COPL+CEPL)) in the Urbión Group varies between 0.6 and 0.9, indicating that compaction can be considered the main process responsible for porosity loss (Figs. 7A and 9). Likewise, different diagenetic pathways of sandstones from the north, centre and south indicate that compaction has most strongly affected the central part of the basin, which has experienced the most subsidence.

5.2.2. Cements and replacements

Several diagenetic precipitates occluded the intergranular pore space. Some of these replace framework components or other cements.

5.2.2.1. Clay Minerals. Kaolinite occurs as pore-filling cement in all areas, occupying intergranular pore space and occasionally as replacement of K-feldspar, generating diagenetic matrix (epimatrix). Its occurrence is highly variable (mean 0.7%, 1.6%, 8.9% in the northern, central and southern areas respectively).

It is possible to distinguish two generations of pore filling, an earlier generation included in the eodiagenesis and a later generation that fills secondary pores. The first pore filling appears to be enclosed by other cements and deformed by mechanical compaction, which suggest an early stage of generation. Eodiagenetic kaolinite is common in warm and wet continental environments (i.e. Worden and Morad, 2003). The last phase shows vadose features and is included in the telodiagenetic stage. It has only been recognized in samples from the southern area of the basin. Telodiagenetic kaolinite must be associated with an influx of low-pH meteoric waters during uplift (Lanson et al., 2002; Ketzer et al., 2003; Worden and Morad, 2003).

Illite appears as pore lining around detrital grains and as replacements of K-feldspar (epimatrix, Fig. 6E). The

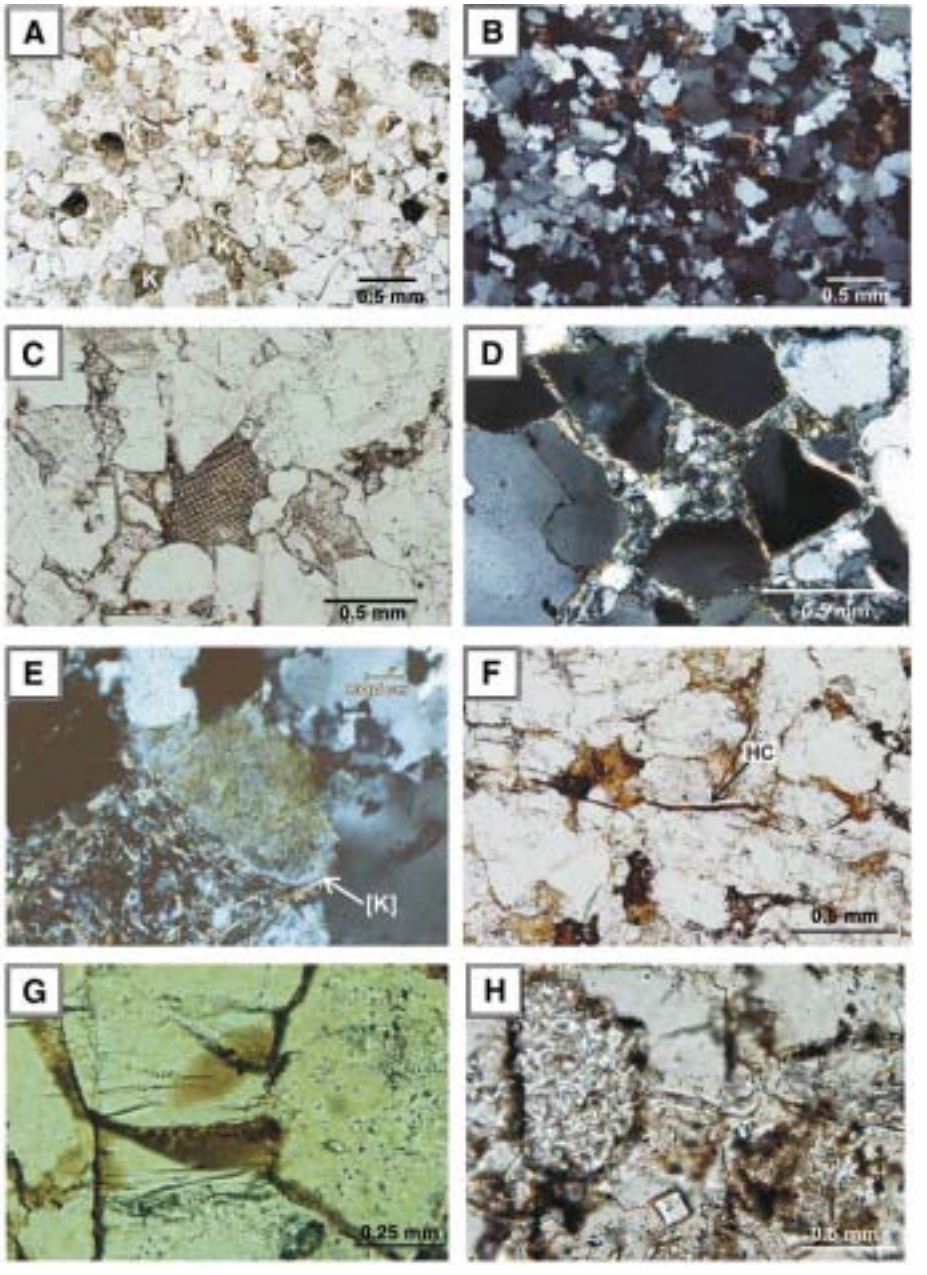

Fig. 6. Thin-section photomicrographs of detrital components and diagenetic features in Urbión Group sandstones. A) Medium-grained sandstone from the southern area of Cameros Basin, showing a quartzose framework with K-feldspar (K) grains. Plane-polarized light. B) Medium-grained quartzarenite from the central area of the basin. The long and concave-convex grain-to-grain contacts suggest that chemical compaction occurred. Cross-polarized light. C) Coarse-grained sublitharenite from the northern area of the basin, exhibiting a well-sorted framework with carbonate grains (echinoid fragment). Plane-polarized light. D) Illite pore lining in a quartzarenite from the northern area. E) K-feldspar cement ([K]) in a very coarse-grained quartzarenite of the central area. Cross-polarized light. F) Fibres of hydrocarbons showing features of deformation. G) Hydrocarbon traces surrounding quartz grains. H) Tiny siderite rhomb suggesting an early diagenetic origin. Note the diagenetic matrix (epimatrix) on the left side, produced by the replacement of a K-feldspar by clay minerals. Plane-polarized light.

pore lining is inferred to be early and related to the eodiagenetic stage. It is generally thin and discontinuous (Fig. 6D). Its occurrence is variable (maximum percentage 13.2%, 15.7% and 2.9%, mean 2.3%, 2.8% and 0.5% in the northern, central and southern areas respectively). The illite pore lining is tangential to grain

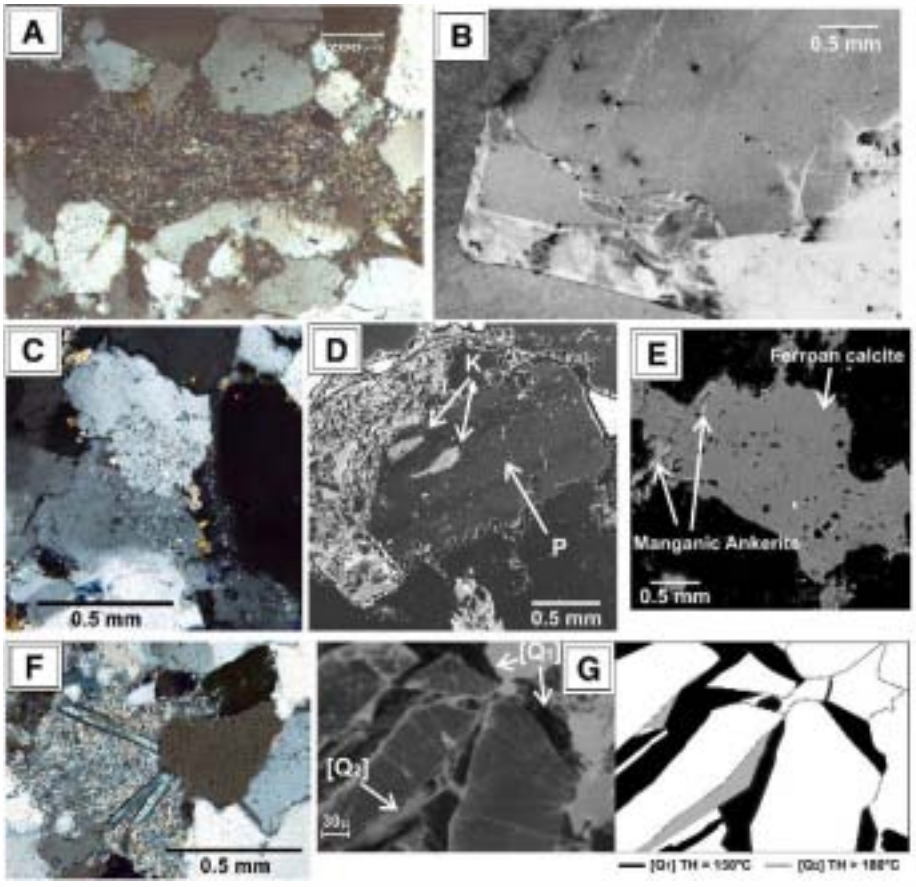

Fig. 7. Thin-section photomicrographs of detrital components and diagenetic features in Urbión Group sandstones. A) Non-carbonate intrabasinal grain (NCI, rip-up clast) deformed by mechanical compaction. Cross-polarized light. B) SEM cathodoluminescence image of a detrital quartz grain with internal zoning in the overgrowth. Note the crushing and microfracturing of the grain before quartz precipitation. C) Quartz replacing a still recognisable K-feldspar grain, cross-polarised light. D) Backscattered image of a plagioclase from a sample in the northern area with relicts of K-feldspar. This could be evidence of albitization. E) Backscattered image of carbonate cement from the central area. F) prismatic chloritoid evidencing a low-grade metamorphic process. Cross-polarized light. G) SEM cathodoluminescence image of detrital quartz grains from the northern area showing two phases of quartz cement. The sketch on the right side better differentiates the two quartz cementation phases.

surfaces. Some illitic coatings are texturally similar to smectite, which suggests a smectite precursor (Morad et al., 1994) that was illitised during diagenesis. Replacement of K-feldspar by illite is considered to have taken place during mesodiagenesis in a relatively closed system at 120 °C–140 °C, and at burial depths greater than 3.7 km (Chuhan et al., 2000, 2001). Illitisation of feldspar pre-dates quartz cementation. It is not clear whether the process continued after precipitation of quartz.

5.2.2.2. K-feldspar. This cement occurs as euhedral, thin and discontinuous overgrowths and is commonly corroded and replaced by illite and carbonate cements (Fig. 6E). It attains 0.5% in all areas of the basin. It is a very early phase, which predates quartz and carbonate cements. This indicates early precipitation in eodiagenetic environments (Fig. 8).

5.2.2.3. Injection of hydrocarbons. The first event of hydrocarbon injection is inferred to have occurred early, because some hydrocarbon fibres lie between quartz grains, pre-dating quartz cements (Fig. 6F and G). The fibres occur as very thin, brown coatings. The presence of these hydrocarbon residues has been confirmed with electron microprobe analysis and with organic solvents. The residues are related to the migration of oil into the reservoir, which took place in the Late Aptian–Early Albian, prior to the hydrothermal event. This migration involved the Cameros Trough and its satellite basins, located to the north and south. Furthermore, Mas et al. (2003) suggest that the tectonic inversion of the basin

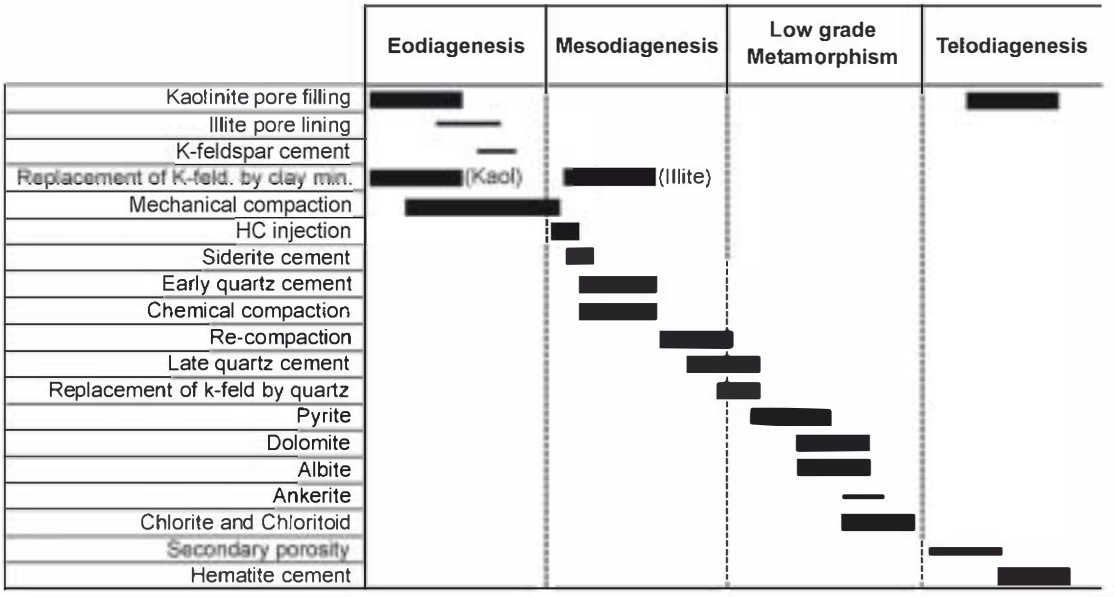

Fig. 8. Chronology of the main post-depositional processes and products ascribed to eodiagenesis, mesodiagenesis, telodiagenesis and to the metamorphic event (shaded zone).

(Eocene–Early Miocene) produced another late migration of hydrocarbons towards satellite basins.

5.2.2.4. Siderite. Siderite occurs as isolated crystals (Fig. 6H) and is considered an early phase, as it is often appears embedded in quartz cement. Siderite precipitation requires a reducing environment related to methanogenesis (e. g. Mozley and Wersin, 1992).

5.2.2.5. Early and late quartz. Quartz is generally the most abundant cement but is variable in abundance. It is mainly developed in the northern and central areas, reaching 9.9% and 12.9% of total rock volume (mean, 2% and 2.8%) respectively.

Diagenetic quartz cement appears as overgrowths around detrital grains, and locally includes other earlier diagenetic phases such as clay minerals (kaolinite and illite) and siderite. Quartz cement typically appears to have been corroded by other minerals (i.e. carbonates). It postdates compaction, which indicates that it precipitated during relatively deep burial (mesodiagenesis, Fig. 8) at depths of more than 2.5 km and temperatures above 80 °C (e.g. Worden and Morad, 2000; Walderhaug et al., 2001).

In addition, quartz cement postdates hydrocarbon emplacement. Although early hydrocarbon emplacement has been cited as a barrier to authigenic quartz nucleation (Worden et al., 1998; Bloch et al., 2002), quartz cementation is possible regardless of the timing of hydrocarbon generation and migration (Reed et al., 2005). Pressure solution, clay mineral reactions in intercalated mudstones, and the dissolution of K-feldspars during burial diagenesis (Bjørlykke and Egeberg, 1993; Barclay and Worden, 2000; Bloch et al., 2002) are likely sources for quartz cement. Quartz cementation is facilitated in the presence of micas, clay minerals and/or organic matter, which release the water necessary to diffuse silica out of the contact zone (Wilson, 1994). Chemical compaction generated quartz cementation prior to the metamorphic peak event.

In addition, the fluid inclusion analysis discussed below indicates the presence of a second quartz cement phase (late quartz in Fig. 8) that is ascribed to the metamorphic event. This phase of quartz cementation is recognizable on cathodoluminescence images as a zonation in the overgrowths (Fig. 7B). The zonations in the quartz overgrowths are due to variations in aluminium and transition metals (Kraishan et al., 2000).

5.2.2.6. Secondary porosity. Secondary porosity is high in the southern area (maximum value of 20.1%, mean 9.2%), and decreases to lower values in the central and northern areas (mean 2.5 and 7.9%, respectively). It is manifested by the presence of corroded grains and partial dissolution and originated by the dissolution of framework grains, mainly K-feldspars and carbonates. Occasionally, secondary pores have developed in intergranular cement.

5.2.2.7. Hematite. Hematite cement occurs as grain coatings or as secondary pore filling. Its occurrence is very variable (mean 1.2%, 1.1% and 3.4% in the northern, central and southern areas respectively). Occurrences of

this cement are typically accompanied by high values of secondary porosity. Hematite cement precipitates under oxidizing conditions and may appear as an early grain coating or as a telodiagenetic product, resulting from de-dolomitization of Fe-rich dolomite at shallow depths (Morad et al., 1995) and pyrite oxidation.

5.2.3. Metamorphic processes and products

In addition to diagenetic processes and products, hydrothermal imprints on the sandstones have been observed in samples from the northern and central areas of the basin.

5.2.3.1. Pyrite precipitation. The percentage of pyrite considered of metamorphic origin ranges from 0.2% to 1.4% in the northern area (mean 0.1%) and from 0.2% to 8.2% (mean 0.9%) in the central area. These pyrite crystals appear as euhedral coarse crystals that cement and replace framework and previous diagenetic products in the sandstones (Alonso-Azcárate et al., 2001). This pyrite is attributed to highly saline waters that produced sulphur mineralisation in the presence of hydrocarbons (Rowe and Burley, 1997; Alonso-Azcárate et al., 2001). Temperatures of 367 °C have been estimated for the precipitation of this mineral (Alonso-Azcárate et al., 1999a).

5.2.3.2. Replacement of K-feldspars by quartz. Replacement of K-feldspars by quartz is common in samples from the central and northern areas (Fig. 7C). It occurs in percentages between 0.2% and 1.6%, in the northern area and between 0.2% and 4.2%, in the central area and is manifested by the presence of illite inclusions on quartz overgrowths that preserve the external shape of precursor K-feldspar grains. This process requires high silica concentrations and high temperatures. For this reason, it must be related to hydrothermal fluids supersaturated in silica.

5.2.3.3. Carbonate cements. Dolomite appears as small rhombic crystals that locally occlude pores. Its content varies from 0.2% to 36.1%. The mean values are 12.5% in the northern area and 1.5% in the central area. Dolomite crystals typically have abundant fluid inclusions that give the cements a turbid aspect in transmitted light. Dolomite cement has a bright cathodoluminescence signal that is explained by anoxic conditions during precipitation (Tucker, 1988). The origin of this dolomite is presumably related to hydrothermal fluids, and postdates the pyrite phase. Later carbonate cements, especially calcite, frequently replaced dolomite cement in the telodiagenetic stage.

Ankerite occurs as isolated patches and is replaced by later calcite cement (Fig. 7E). Ankerite cement occupies such a low percentage of intergranular volume that it has not been quantified. In the central part of the basin, ankerite has bright luminescence (Fig. 7E) and high values of Mn (manganic ankerite). In many cases, the trace-element content of late diagenetic carbonate cements is depleted in iron and magnesium, and enriched in manganese (Lynch and Land, 1996; Milliken, 1998). Alternatively the high Mn values can be generated by hydrothermal flow (Chow et al., 1996; Morad et al., 2000).

5.2.3.4. Albitization. The presence of twinned and untwinned albite in the northern and central areas of the basin suggests that albitization took place. The albites appear as fresh idiomorphic and subidiomorphic grains, and sometimes have textural evidence of K-feldspar replacement (Fig. 7D). The composition of authigenic albite is close to the Na end member and is largely non-luminescent (Kastner and Siever, 1979). Albitization predates several carbonate cementation phases and is common as a replacement in depths greater than 2500 m, especially in sandstones rich in K-feldspars (Morad et al., 1990). The Na required for albitization is probably derived from dissolution of Triassic evaporites (Saigal et al., 1988).

5.2.3.5. Chlorite and chloritoid. A metamorphic event is also inferred from the presence of two metamorphic minerals, chlorite and chloritoid, in samples from the northern and central areas of the basin (Fig. 7F). The content of chlorite varies from 0.2% to 4.2% (mean 1.5%) in the northern area and from 0.2% to 10% (mean 2%) in the central area.

Chlorite replaces quartz, K-feldspars and micas. It appears on argillaceous framework grains (intrabasinal grains and metamorphic rock fragments) and is associated with clay minerals from the sandstone matrix. Diagenetic chlorite is recognized as polycrystalline micronodules or as radial aggregates. The content of chloritoid reaches 2.4% (mean 0.4%). It appears as tabular crystals or in aggregates. It is possible that these crystals retrograde into chlorite whilst maintaining their previous morphology (pseudomorphosis).

5.3. The imprint of hydrothermal processes on quartz overgrowths

Under transmitted light, quartz overgrowths are generally 20 to 40 μm thick and display uniform extinction. Two types of quartz cement can be recognized under SEM-CL, which will be referred to as cathodoluminescence zones Q1 and Q2. These two cements occur together in different samples from the northern and central areas of the basin.

Q1 (Fig. 7G) is dark under CL and it preserves "ghosts" of fibrous structure that are perpendicular to the detrital grain-overgrowth boundary. Q2 is bright and has concentric growth zoning (Fig. 7B) or is isopachous. Locally, this cement displays irregular boundaries inconsistent with growth and has a patchy distribution. The dark Q1 cement has been fractured and its spaces filled with bright Q2. Fragments of Q1 are frequently included in the Q2 cement. The destruction of the original texture of Q1 cements is probably due to high-temperature recrystallization (Goldstein and Rossi, 2002). Hence, the hot hydrothermal fluids that generated the bright Q2 cement are likely to have caused the recrystallization of Q1 as well. In contrast, Q1 cement is less common in sandstones from the central area and where it appears is thin and discontinuous. This could also be related to the predominance of hydrothermal processes, which lowered the preservation potential of Q1 in the central area relative to the northern area.

Homogenization temperatures were measured in syntaxial quartz overgrowths in sandstones from the northern and central areas. Two types of fluid inclusions were observed in distinct parts of quartz overgrowths, as shown by SEM-associated cathodoluminescence images. One type of fluid inclusion (the first generation) occurs in the dark, non-luminescent phase (Q1), closest to the detrital grain-overgrowth boundary. It was formed at low temperatures (from 100.5 °C to 115 °C, mean 110 °C), and is interpreted to have a diagenetic origin. The other type of fluid inclusion (the second generation) is included in bright and more luminescent cements (Q2, Fig. 7G), further away from detrital grain-overgrowth boundaries. It was formed at higher temperatures (from 95 °C to 227 °C, mean 175 °C), and is considered to be of hydrothermal origin (Fig. 9). We propose that the high temperatures reflect the injection of hydrothermal fluids whereas the low temperatures reflect maximum burial. The spatial distribution of the two types of inclusions and their temperatures of formation indicate that the Q2 phase is of hydrothermal origin.

The first cement (Q1) precipitated from a single fluid reservoir, because salinity values are homogeneous within each sample, whereas the fluid inclusions with higher temperatures are inferred to correspond to a mixture of two fluid reservoirs, recognized by different salinity values for similar homogenization temperatures (Th) in the same sample. For Th = 100 °C, salinity values between 3.4 and 6.2 ‰ were registered. These reservoirs could have been affected by the hydrothermal metamorphism related to the rifting evolution (Casquet et al., 1992; Barrenechea et al., 1995).

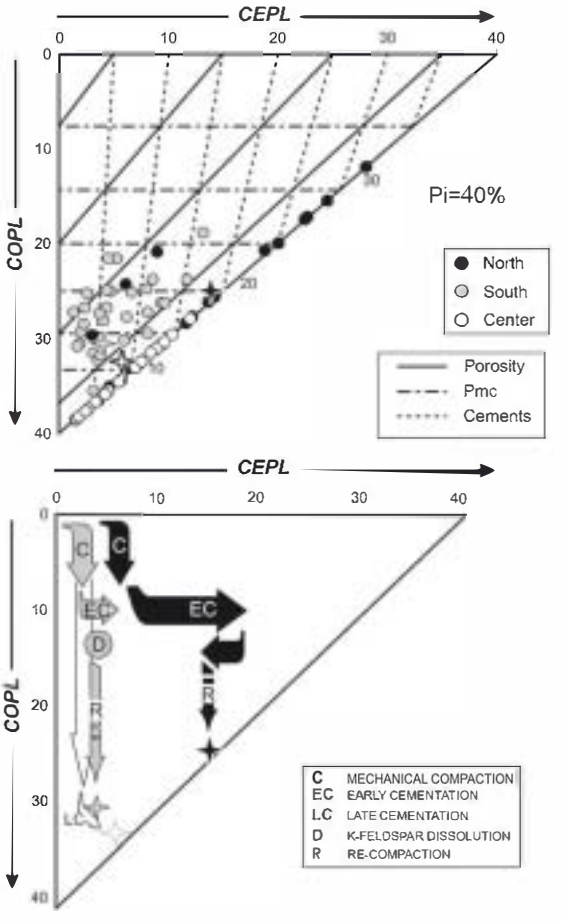

Fig. 9. Diagenetic paths diagrams showing the loss of porosity by cementation processes (CEPL) *versus* compaction processes (COPL) of the studied sandstones in the southern, central and northern areas of the basin, according to Lundegard (1992).

The circulation of hydrothermal fluids took place after the basin was filled. This suggests that hydrothermal activity was not restricted to the deepest part of the basin (Barrenechea et al., 2001). The maximum temperatures did not exceed 340 °C (highest metamorphic conditions) and the pressure remained below 1.0 Kb (around 3.5 to 4 km deep). Fluid circulation could have been enhanced by extensional fractures, sedimentary discontinuities and the relatively high permeability of the deposits (Alonso-Azcárate et al., 1999a).

6. Discussion

Although petrofacies vary from south (quartzofeldspathic) to north (quartzose and quartzolithic, respectively), all sandstones from the Urbión Group in the Cameros Basin had a rigid framework with high original porosity values at the time of deposition. Textural

maturation of sediments during transport and intense weathering produced moderately to well-sorted sandstones with a quartzose framework. The presence of primary porosity in some samples from the northern and southern areas indicates that conduits for fluid flow were not completely eliminated during burial. Together, these features suggest that the fluvial sandstones were originally a high-quality reservoir. Unfortunately, diagenetic and metamorphic processes degraded these original characteristics. Diagenetic processes reduced original porosity by intense compaction (COPL) and cementation (CEPL). Concavo-convex contacts, which indicate pressure solution, are common. Mechanical and chemical compaction was the most important mechanism of porosity reduction in the basin.

Several cementation phases have been distinguished. Pore-filling kaolinite, pore-lining illite and K-feldspar cements were recognized. These cementation phases started to fill the intergranular pores in the eodiagenetic stage. Petrographic observations suggest that kaolinite formed at shallow depth. An influx of fresh water is a likely explanation for its origin (Bjørlykke, 1998). K-feldspar overgrowths formed at relatively shallow burial depths. K-feldspar precipitation requires high silica activities and high K^+/H^+ ratios (Morad et al., 2000) and the occurrence of feldspar overgrowths may imply that detrital feldspars were dissolving (De Ros et al., 1994). Generation and migration of hydrocarbons occurred during early mesodiagenesis. Today, this is recognizable by the presence of carbon residues appearing as thin fibres, locally showing deformation features. These are the result of mixing of hydrocarbons with subsequent hydrothermal fluids, which generated a carbon residue and triggered water release.

In addition, in the mesodiagenetic realm, a re-compaction event took place that induced breakage of clasts and previous cements by framework collapse, and reduced the porosity (Figs. 7B and 10). Re-compaction has been inferred only in samples from the northern and southern areas of the basin, in which sufficient K-feldspar and carbonate cement were present to promote framework collapse by dissolution. Thus, porosity reduction is proposed to have occurred in four stages (Fig. 9): (1) Loss of primary porosity by early mechanical compaction; (2) early cementation, mainly by kaolinite and K-feldspar; (3) dissolution of framework grains in the southern area and dissolution of carbonates in the northern area; and (4) framework collapse by re-compaction.

The diagenetic trend of sandstones from the central area is different, for many reasons. Firstly, there are not as many K-feldspars that are prone to dissolution, so re-

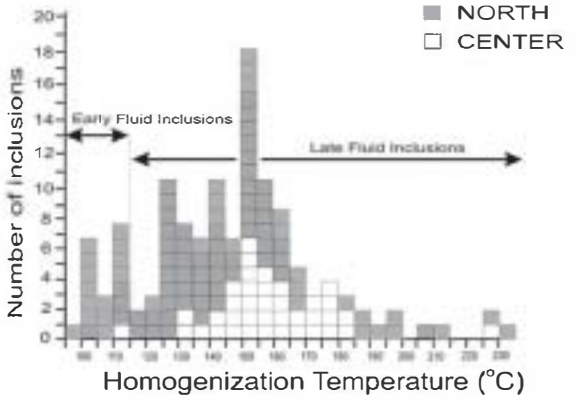

Fig. 10. Histograms of homogenisation temperatures in primary fluid inclusions in quartz overgrowths. Notice the two populations of fluid inclusion homogenisation temperatures.

compaction did not take place. Secondly, the central area experienced the most subsidence, which means that compaction has been greatest there. Also, quartz cement seems to be the main cause of porosity reduction in the central area relative to the northern and southern areas. Carbonate cementation has been of minor importance for porosity reduction. The diagenetic trend implies constant compaction with minimal carbonate cementation.

In the northern and central areas of the basin, hydrothermal metamorphism destroyed reservoirs and caused a second generation of quartz overgrowths and replacement of K-feldspar by quartz, in addition to carbonate cementation (including dolomite and ankerite), albitization, and precipitation of pyrite and chlorite-chloritoid. All these processes are consistent with the presence of fluids supersaturated in silica, which are typical of hydrothermal systems (Fournier, 1985). Moreover, according to Alonso-Azcárate et al. (1999a), the estimated temperatures for pyrite precipitation are consistent with the hydrothermal metamorphic realm.

Textural and fluid inclusion evidence indicates that precipitation of silica of diagenetic and metamorphic origin occurred throughout the burial history. Temperatures deduced from fluid inclusion analysis in the second generation of quartz overgrowths of metamorphic origin range from 95 °C to 227 °C, which is compatible with the maximum temperature of 340 °C proposed by Casquet et al. (1992) for the metamorphic peak. The hydrothermal phase that affected the Cameros Trough also destroyed the hydrocarbon charge and the porosity of the reservoirs. Nevertheless, those hydrocarbons that migrated early from the Cameros depocentre towards the margins of the basin may have been preserved, as they were not affected by hydrothermal metamorphism (Mas et al., 2003). Thus, sufficient permeability and intergranular volume must

have been preserved in "rigid-grain" sandstones, despite significant burial.

The final processes that affected the Urbión Group rocks are related to telodiagenesis, and include the generation of secondary porosity, cementation of haematite, oxidation of pyrites, and replacement of dolomite by calcite. All these processes were more intense in the northern and southern areas than in the central area, possibly because circulation of meteoric waters was slower in the central area of the basin, due to the lower porosity values of the hydrothermally altered sandstones.

7. Conclusions

1. The dispersal systems that fed the Cameros Basin produced large volumes of sands with quartz-rich petrofacies during sedimentation of the Urbion Group. Their rigid framework and low matrix content promoted high primary porosity values favourable for a high-quality reservoir.
2. The provenance of the sandstones has influenced diagenesis mainly by controlling the spatial distribution of K-feldspars. The most important diagenetic processes are compaction (mechanical and chemical) and cementation by kaolinite, siderite and quartz. Hydrocarbon emplacement occurred before quartz cementation.
3. Diagenetic processes related to hydrothermal metamorphism significantly reduced porosity and destroyed all reservoir potential in the Cameros Trough. Dominant processes were re-compaction, late quartz and carbonate cementation, and growth of chlorite, chloritoid and pyrite.
4. The preservation of hydrocarbons in peripheral and satellite basins supports the idea that the Urbión Group is a good potential hydrocarbon reservoir in locations not affected by hydrothermal processes.
5. This study in the Cameros Basin may serve to reassess the possibility of finding potential clastic reservoirs in intracratonic rift basins, despite the likely presence of locally destructive effects on reservoir quality produced by clastic diagenesis and low-grade hydrothermal metamorphism.

Acknowledgements

Founding for this research was provided by the Spanish DIGICIT projects BTE2001-026 and CGL2005-07445-C03-02/BTE. This manuscript has been improved by comments and suggestions from G.J. Weltje and four anonymous referees.

Appendix A. Supplementary data

Supplementary data associated with this article can be found, in the online version, at doi:10.1016/j.sedgeo.2007.05.017.

References

Alonso-Azcárate, J., Barrenechea, J.F., Rodas, M., Mas, J.R., 1995. Comparative study of the transition between very low-grade and low-grade metamorphism in siliciclastic and carbonate sediments: early Cretaceous, Cameros Basin (Northern Spain). Clay Minerals 30, 407–419.

Alonso-Azcárate, J., Rodas, M., Bottrell, S.H., Raiswell, R., Velasco, F., Mas, R., 1999a. Pathways and distances of fluid flow during low-grade metamorphism: evidence from pyrite deposits of the Cameros Basin, Spain. Journal of Metamorphic Geology 17, 339–348.

Alonso-Azcárate, J., Rodas, M., Bottrell, S.H., Mas, J.R., Raiswell, R., 1999b. Estudio textural e isotópico de los sulfuros diseminados en los sedimentos de la cuenca de Cameros (La Rioja, España). Revista de la Sociedad Geológica de España 12, 241–249.

Alonso-Azcárate, J., Rodas, M., Fernández-Díaz, L., Bottrell, S.H., Mas, R., López-Andrés, S., 2001. Causes of variation in cristal morphology in metamorphogenic pyrite deposits of the Cameros Basin (N of Spain). Geological Journal 36, 159–170.

Arribas, J., Mas, R., Alonso, A., Ochoa, M., 2003. Diagenetic processes controlling the quality of potential clastic reservoirs in a continental rift basin: western Cameros Basin, Spain. AAPG International Conference and Exhibition, Barcelona, Spain, (Poster presentation).

Barclay, S.A., Worden, R.H., 2000. Effects of reservoir wettability on quartz cementation in oil fields. In: Worden, R.H., Morad (Eds.), Quartz cementation in sandstone reservoirs. Special Publication of the International Association of Sedimentologists, vol. 29, pp. 103–117.

Barrenechea, J.F., Rodas, M., Mas, J.R., 1995. Clay mineral variations associated with diagenesis and low-grade metamorphism of early Cretaceous sediments in the Cameros Basin, Spain. Clay Minerals 30, 119–133.

Barrenechea, J.F., Rodas, M., Frey, M., Alonso-Azcárate, J., Mas, J.R., 2001. Clay diagenesis and low grade metamorphism of Tithonian and Berriasian sediments in the Cameros Basin (Spain). Clay Minerals 36, 325–333.

Beard, D.C., Weyl, P.K., 1973. Influence of texture on porosity and permeability of unconsolidated sand. American Association of Petroleum Geologists Bulletin 57, 349–369.

Bjørlykke, K., 1998. Clay mineral diagenesis in sedimentary basins: a key to the prediction of rock properties. Examples from the North Sea Basin. Clay Minerals 33, 15–34.

Bjørlykke, K., Egeberg, P.K., 1993. Quartz cementation in sedimentary basins. American Association of Petroleum Geologists Bulletin 77, 1536–1548.

Bloch, S., Lander, R.H., Bonnell, L., 2002. Anomalously high porosity and permeability in deeply buried sandstone reservoirs: origin and predictability. American Association of Petroleum Geologists Bulletin 86, 301–328.

Buick, R., Rasmussen, B., Krapez, B., 1998. Archean oil: evidence for extensive hydrocarbon generation and migration 2.5-3.5 Ga. American Association of Petroleum Geologists Bulletin 82, 50–69.

Casquet, C., Galindo, C., González-Casado, J.M., Alonso, A., Mas, J.R., Rodas, M., García, E., Barrenechea, J.F., 1992. El metamorfismo en

la cuenca de los Cameros. Geocronología e implicaciones tectónicas. Geogaceta 11, 22–25.

Chayes, F., 1952. Notes of the staining of potash feldspar with sodium cobaltinitrite in thin section. The American Mineralogy 37, 337–340.

Chow, N., Morad, S., Al-Aasm, I.S., 1996. Origin of authigenic carbonates in Eocene to Quaternary sediments from the Arctic and Norwegian-Greenland Sea. In: Myhre, A., Thiede, J., Firth, J., Ruddiman, W.F., Johnsson, L. (Eds.), Proceedings of the Ocean Drilling Program, Scientific Results, vol. 151, pp. 415–434.

Chuhan, F.A., Bjorlykke, K., Lowrey, C., 2000. The role of provenance in illitization of deeply buried reservoir sandstones from Haltenbanken and North Viking Graben, offshore Norway. Marine and Petroleum Geology 17, 673–689.

Chuhan, F.A., Bjorlykke, K., Lowrey, C.J., 2001. Closed-system burial diagenesis in reservoir sandstones; examples from the Gam Formation at Haltenbanken area, offshore Mid-Norway. Journal of Sedimentary Research 71, 15–26.

De Ros, L.F., Sgarbi, G.N., Morad, S., 1994. Multiple authigenesis of K-feldspar in sandstones; evidence from the Cretaceous Areado Formation, Sao Francisco Basin, central Brazil. Journal of Sedimentary Research 64, 778–787.

De Ros, L.F., Morad, S., Broman, C., De Césereo, P., Gomez-Gras, D., 2000. Influence of uplift and magmatism on distribution of quartz and illite cementation: evidence from Siluro-Devonian sandstones of the Paraná Basin, Brazil. Special Publication of the International Association of Sedimentologists 29, 231–252.

Dickinson, W.R., 1985. Provenance relations from detrital modes of sandstones. In: Zuffa, G.G. (Ed.), Provenance of arenites. NATO ASI Series, vol. C-148, pp. 333–362.

Dutkiewicz, A., Rasmussen, B., Buick, R., 1995. Oil preserved in fluid inclusions in Archaean sandstones. Nature 395, 885–888.

Fournier, R.L., 1985. The behaviour of silica in hydrothermal solutions. In: Berger, B.R., Bethke, P.M. (Eds.), Geology and Geochemistry of Epithermal Systems: Society of Economic Geologists. Reviews in Economic Geology, vol. 2, pp. 45–61.

Goldstein, R.H., Reynolds, T.J., 1994. Systematics of fluid inclusions in diagenetic minerals. SEPM Short Course, vol. 31. SEPM, Tulsa. 199 pp.

Goldstein, R.H., Rossi, C., 2002. Recrystallization in quartz overgrowths. Journal of Sedimentary Research 72, 432–440.

Guimerá, J., Alonso, A., Mas, R., 1995. Inversion of an extensional ramp basin by a newly formed thrust: the Cameros basin (N Spain). In: Buchanan, J.G., Buchanan, P.G. (Eds.), Basin Inversion. Geological Society of London Special Publication, vol. 88, pp. 433–453.

Hoffman, J., Hower, J., 1979. Clay mineral assemblages as low grade metamorphic geothermometers: Application to the thrust faulted disturbed belt of Montana, U.S.A. SEPM Special Publication 26, 55–79.

Houseknecht, D.W., 1987. Assessing the relative importance of compaction processes and cementation to reduction of porosity in sandstones. American Association of Petroleum Geologists Bulletin 71, 633–642.

Ingersoll, R.W., Bullard, T.F., Ford, R.L., Grimm, J.P., Pickle, J.D., Sres, S.W., 1984. The effect of grain size on detrital modes: a test of the Gazzi-Dickinson point counting method. Journal of Sedimentary Petrology 54, 103–116.

Kastner, M., Siever, R., 1979. Low temperature feldspars in sedimentary rocks. American Science 279, 435–479.

Ketzer, J.M., Morad, S., Amorosi, A., 2003. Predictive clay cementation in a sequence stratigraphy framework. In: Worden, R.H., Morad, S. (Eds.), Clay Cementation in sandstones. International Association of Sedimentologists, Special Publication, vol. 34, pp. 42–59.

Kraishan, G.M., Rezaee, M.R., Worden, R.H., 2000. Significance of trace element composition of quartz cement as a key to reveal the origin of silica in sandstones: an example from the Cretaceous of the Barrow Sub-basin, Western Australia. In: Worden, R.H., Morad, S. (Eds.), Quartz Cementation in sandstones. International Association of Sedimentologists, Special Publication, vol. 29, pp. 317–331.

Lanson, B., Beaufort, D., Berger, G., Bauer, A., Cassagnabère, A., Meunier, A., 2002. Authigenic kaolin and illite minerals during burial diagenesis of sandstones: a review. Clay Minerals 37, 1–22.

Larese, R.E., 1997. Impact of diagenetic processes on sandstone reservoir quality; controls, effects, and predictive evaluation using data from natural and experimental systems. American Association of Petroleum Geologists Bulletin 81, 1955.

Lindholm, R.C., Finkelman, R.B., 1972. Calcite staining; semiquantitative determination of ferrous iron. Journal of Sedimentary Petrology 42, 239–245.

Lundegard, P.D., 1992. Sandstone porosity loss — a "big picture" view of the importance of compaction. Journal of Sedimentary Petrology 62, 250–260.

Lynch, F.L., Land, L.S., 1996. Diagenesis of calcite cement in Frio Formation sandstones and its relationship to formation water chemistry. Journal of Sedimentary Research 66, 439–446.

Mantilla, L.C., Casquet, C., Mas, R., 1998. Los paleofluidos en el Grupo Oncala, Cuenca de Cameros (La Rioja, España): datos de inclusiones fluidas, isótopos de oxígeno y SEM. Geogaceta 24, 207–210.

Mantilla, L.C., Casquet, C., Galindo, C., Mas, R., 2002. El metamorfismo hidrotermal cretácico y paleógeno en la cuenca de Cameros (Cordillera Ibérica, España). Revista Zubía, Monográfico 14, 143–154.

Mas, R., Alonso, A., Guimerá, J., 1993. Evolución tectonosedimentaria de una cuenca extensional intraplaca: la cuenca finijurásica-eocretácica de Los Cameros (La Rioja–Soria). Revista de la Sociedad Geologica de España 6 (3–4), 129–144.

Mas, R., Benito, M.I., Arribas, J., Serrano, A., Guimerá, J., Alonso, A., Alonso-Azcárate, J., 2002. La cuenca de Cameros: desde la extensión finijurásica-eocretácica a la inversión terciaria -implicaciones en la exploración de hidrocarburos-. Zubía Monográfico 14, 9–64. Logroño.

Mas, R., Benito, M.I., Arribas, J., Serrano, A., Guimerá, J., Alonso, A., Alonso-Azcárate, J., 2003, The Cameros Basin: From Late Jurassic–Early Cretaceous Extensión to Tertiary Contractional Inversión–Implications of Hydrocarbon Exploration. Northwest Iberian Chain, North Spain. Geol. Field Trip, 11, AAPG International Conference and Exhibition. Barcelona, Ed. Cent. Recherches. Elf-Total-Fina. 56p.

Mata, M.P., Casas, A.M., Canals, A., Gil, A., Pocoví, A., 2001. Termal history during Mesozoic extendion and Tertiary uplift in the Cameros Basin, northern Spain. Basin Research 13, 91–111.

Milliken, K.L., 1998. Carbonate diagenesis in non-marine foreland sandstones at the western edge of the Alleghanian overthrust belt, southern Appalahians. In: Morad, S. (Ed.), Carbonate Cementation in Sandstones. International Association of Sedimentologists Special Publication, vol. 26, pp. 87–105.

Montigny, R., Azambre, B., Rossy, M., Thuizat, R., 1986. K-Ar study of Cretaceous magmatism and metamorphism in the Pyrenees; age and length of rotation of the Iberian Peninsula. Tectonophysics 129, 257–273.

Morad, S., Bergan, M., Knarud, R., Nystuen, J.P., 1990. Albitization of detrital plagioclase in Triassic reservoir sandstones from the Snorre Field, Norwegian North Sea. Journal of Sedimentary Petrology 60, 411–425.

Morad, S., Ben Ismail, H., De Ros, L.F., Al-Aasm, I.S., Serrihini, N.E., 1994. Diagenesis and formation water chemistry of Triassic reservoir sandstones from southern Tunisia. Sedimentology 41, 1253–1272.

Morad, S., Al-Aasm, I.S., Longstaffe, F.J., Marfil, R., De Ros, L.F., Johansen, H., Marzo, M., 1995. Diagenesis of a mixed siliciclastic/evaporitic sequence of the middle Muschelkalk (Middle Triassic), the Catalan Coastal Range, NE Spain. Sedimentology 42, 749–768.

Morad, S., Ketzer, J.M., De Ros, F., 2000. Spatial and temporal distribution of diagenetic alterations in siliciclastic rocks: implications for mass transfer in sedimentary basins. Sedimentology 47, 95–120.

Mozley, P.S., Wersin, P., 1992. Isotopic composition of siderite as an indicator of depositional environment. Geology 20, 817–820.

Ochoa, M., Arribas, J., Mas, R., 2004. Changes in sandstone composition during Lower Cretaceous syn–rift fluvial sedimentation (Cameros Basin, Spain). 32nd International Geological Congress, Florence (Italy). Abstract CD, Session 242–34.

Oelkers, E.H., Bjørkum, P.A., Murphy, W.M., 1996. A petrographic and computational investigation of quartz cementation and porosity reduction in North Sea sandstones. American Journal of Science 296, 420–452.

Olivet, J.L., Bonnin, J., Beuzart, P., Auzende, J.M., 1984. Cinématique de l'Atlantique nord et central. CNEXO. Rapport Scientifique et Technique 54, 1–108.

Pitman, J.K., Spölt, Ch., 1996. Origin and timing of carbonate cements in the St. Peter Sandstone, Illinois Basin: evidence for a genetic link to Mississippi Valley-type mineralization. SEPM Special Publication 55, 187–203.

Rat, P., 1982. Factores condicionantes en el Cretácico de España. Cuadernos de Geología Ibérica 8, 1059–1076.

Reed, J.S., Eriksson, K.A., Kowalewski, M., 2005. Climatic, depositional and burial controls on diagenesis of Appalachian Carboniferous sandstones: qualitative and quantitative methods. Sedimentary Geology 176, 225–246.

Rowe, J.E., Burley, S.D., 1997. Fault-related diagenetic cementation in Triassic Sandstones at Alderley Edge, north-eastern Cheshire. In: Meadows, N., Cowan, G. (Eds.), Petroleum Geology of the Irish Sea and its Margins. Geological Society of London, Special Publication, vol. 124, pp. 325–352.

Saigal, G.C., Morad, S., Bjørlykke, K., Egeberg, P.K., Aagaard, P., 1988. Diagenetic albitization of detrital K-feldspars in Jurassic, Lower Cretaceous, and Tertiary clastic reservoir rocks from offshore Norway, I. Textures and origin. Journal of Sedimentary Petrology 58, 1003–1013.

Salas, R., Guimerá, J., Mas, J.R., Martín-Closas, C., Meléndez, A., Alonso, A., 2001. Evolution of the Mesozoic Central Iberian Rift System and its Cenozoic inversión (Iberian Chain). In: Cavazza, W., Robertson, A., Ziegler, P. (Eds.), Peri-Tethyan Rift/Wrench Basins and Passive Margins. Mémoires du Muséum National d'Histoire Naturelle, vol. 186, pp. 145–185.

Salinas, F.J., Mas, J.R., 1989. Individualización de la cubeta lacustre de Cervera del Río Alhama (la Rioja) durante la sedimentación del Grupo Urbión (Cretácico inferior). Comunicaciones, XII, Congreso Español de Sedimentología, Bilbao, pp. 79–82.

Spötl, C., Houseknecht, D.W., Longstaffe, F.J., 1994. Authigenic chlorites in sandstones as indicators of high-temperature diagenesis, Arkoma foreland basin, USA. Journal of Sedimentary Research 64, 553–566.

Spötl, C., Houseknecht, D.W., Riciputi, L.R., 2000. High-temperature quartz cement and the role of stylolites in a deep gas reservoir, Spiro Sandstone, Arkoma Basin, USA. International Association of Sedimentologists Special Publication 29, 281–297.

Tissot, B.P., Welte, D.H., 1978. Petroleum formation and occurrence. A New Approach to Oil and Gas Exploration. Springer, Berlin. 538 pp.

Tucker, M., 1988. Techniques in Sedimentology. Blackwell Scientific Publications. 394 pp.

Walderhaug, O., Bjorkum, P.A., Nadeau, P.H., Langnes, O., 2001. Quantitative modelling of basin subsidence caused by temperature-driven silica dissolution and reprecipitation. Petroleum Geoscience 7, 107–113.

Wilson, M.D., 1994. Reservoir quality assessment and prediction in clastic rocks. SEPM Short Course 30. 432 pp.

Worden, R.H., Morad, S. (Eds.), 2000. Quartz cementation in sandstone reservoirs. Special Publication of the International Association of Sedimentologists, vol. 29, pp. 103–117.

Worden, R.H., Morad, S., 2003. Clay mineral cements in sandstones. International Association of Sedimentologists Special Publication 34. 509 pp.

Worden, R.H., Oxtoby, N.H., Smalley, P.C., 1998. Can oil emplacement stop quartz cementation in sandstones? Petroleum Geoscience 4, 129–137.

Zuffa, G.G., 1980. Hybrid arenites: their composition and classification. Journal of Sedimentary Petrology 50, 21–29.